Wireless sensor network-based solution for environmental monitoring: water quality assessment case study

Octavian Postolache[1], José Dias Pereira[2], Pedro Silva Girão[3]

[1]Instituto de Telecomunicações, DCTI/ISCTE-IUL, Lisbon, Portugal
[2]Instituto de Telecomunicações, DSI/EST/IPS, Setubal, Portugal
[3]Instituto de Telecomunicações, DEEC/IST/UL, Lisbon, Portugal
E-mail: opostolache@lx.it.pt

Abstract: The challenges of climate change, population growth, demographic change, urbanization and resource depletion mean that the world's great cities need to adapt to survive and thrive over the coming decades. Slashing greenhouse gas emissions to prevent catastrophic climate change, while maintaining or increasing quality of life, can be a costly and difficult process. Two factors that directly affect the life quality in the XXI century cities are the water and air quality that can be monitored using the combination of low cost sensing modules, machine to machine (M2M) and internet of things (IoT) technologies. In this context, this study presents a wireless sensor network architecture that combines low cost sensing nodes and a low cost multi-parameters sensing probe for reliable monitoring of water quality parameters of surface waters (lakes, estuaries and rivers) in urban areas. A particular attention is dedicated to the design of the conductivity, temperature and turbidity signal conditioning circuits, highlighting important issues related to linearisation, measuring dynamic range and low-cost implementation by using commercial off-the-shelf components and devices. Several issues related to the wireless sensor network implementation are included in this study, as well as several simulation and experimental results.

1 Introduction

Smart cities, in the current worldwide information and communication technology applications scenario, imply a constantly growing number of ever more powerful internet connected devices (smartphones, sensors, household appliances, radiofrequency identification (RFID) devices and so on) and an increasing use of low cost sensors that can deliver information to increase the quality of life. Concerning the concept of smart cities, different approaches are presented in the literature. One of these approaches, developed by IBM [1], includes several pillars, some of them related with environmental monitoring, energy and water, healthcare and smarter buildings, among others. In this context, water resources are a limited resource that requires a careful use, and monitoring its quality is a very important task, regardless of the purpose for which water is used. Thus, the development of ubiquitous solutions for water quality (WQ) assessment will have a huge application in the future, and low-cost sensing solutions and wireless sensing networks must be developed to integrate measurement data. Concerning personalised health care, indoor and outdoor air quality are also important parameters that can be used for instance to correlate clinical data with environmental conditions. Moreover, respiratory distress is the second most common symptom of adults transported by ambulance and is associated with a relatively high overall mortality, of 18%, before hospital discharge [2–4]. Several solutions have been proposed in the area of air quality monitoring [5–7]. Measuring systems to monitor the concentration of gases such as NO_2, CO and the evolution of physical parameters such as relative humidity (RH) and temperature [8, 9] have been deployed.

Air quality and surface WQ should often be considered together because of the relation between them. The best example of a direct link between air pollution and water pollution is acid rain. Acidic gases (NO_x and SO_x) are emitted into the air by various sources. They combine with water in the air to form sulphurous and nitrous acids which then fall as rain to contaminate water in rivers and lakes by decreasing the pH [10, 11]. The acidic water leaches metals out of the rocks and sediments as soluble ions. These increase heavy metal (arsenic, lead and so on) levels in the water. Taking into account these interrelations and also the health protection of the people that use the water for daily activity and for recreation, the existence of distributed measuring systems for on-line monitoring of the quality of water with capability to transmit the information using client-server architectures, including mobile technology, still represents a challenge nowadays.

Considering the example of air quality sensor architectures that were deployed in different cities in the last years [12], one of the conditions to assure a quick implementation is low price of the system. Another important condition is the

capability of the system of monitoring the environment parameters in extended areas. In this context, we considered the development of a system that can provide information about the changes in the quality of water through the measurement of electrical conductivity, temperature and turbidity. Through the measurements of these variables we can detect changes in water environments and study if the causes of those modifications are natural or not, like in the case of pollution. For extended information about the WQ when pollution events are detected, it shall be possible to add to the system multi-parameter WQ probes such as Hydrolab Quanta Multiparameter Sonde [13] or the Rosemount Analytical Model 1057 Multiparameter Analyser [14] for higher flexibility and interoperability.

Taking into account the above mentioned considerations, a WQ sensing module with conductivity, temperature and turbidity measuring channels was designed and implemented. Each sensing module is attached to a wireless sensor node equipped with primary data processing and wireless communication capabilities.

Referring to the conductivity measuring channel, a two electrode cell was used because of its simplicity, but also because it is easy to clean and it covers the desired measuring range 0.1–20 mS/cm [15]. The temperature compensation associated to the conductivity measuring probe is based on the temperature information delivered by the temperature measuring channel that is expressed by a negative temperature coefficient (NTC) thermistor and an appropriate conditioning circuit. The turbidity measuring channel was materialised using two detectors associated with the measurement of transmitted and scattered light emitted by a light source [16].

The signals provided by the measuring channels are acquired, processed and transmitted by an NI-WSN (wireless sensor module) sensor node from National Instruments, through a gateway to a host computer internet connection that provides a WQ monitoring service using LabVIEW web server capabilities. Several signal processing algorithms can be implemented on the host computer including global representation of WQ evolution for the monitored area, pollution events signalling, short term and long term WQ prediction.

2 WQ sensing node and networking

The sensing module associated to each node of the wireless sensor network for urban WQ monitoring is able to measure water electrical conductivity, temperature and turbidity and is connected to the NI analogue input block of the NI WSN-3202 (Fig. 1).

The four bidirectional digital channels that are included in the NI-WSN can be used for several purposes, such as, defining the gain of the signal conditioning programmable gain amplifiers or to supervise faulty conditions of the measuring system, like low supply voltage amplitude or voltage pin amplitudes out of scale. Others important characteristics of the NI-WSN node that dictate its choice include a very low-power consumption, being possible to achieve 3 year of autonomy using 4 AA batteries, a maximum bit rate and sample rate of 250 kbit/s and 1 S/s, respectively, 300 m wireless coverage range without repeaters, and interoperability with others wireless devices such as routers and gateways. It is also important to underline that an outdoor enclosure can be used in each sensing node in order to improve its reliability, which is a
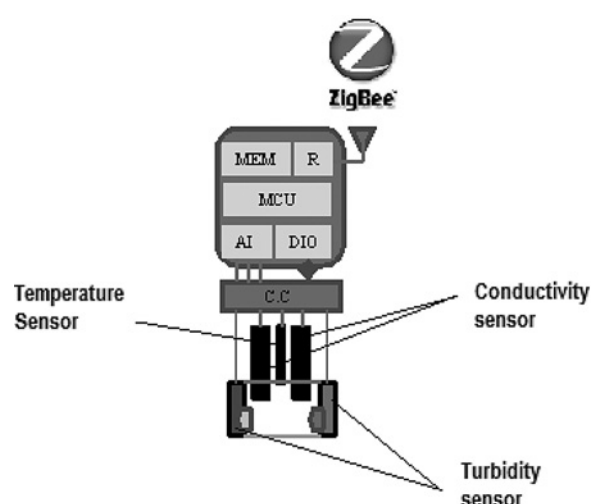

Fig. 1 *Block diagram of the WQ sensing node*
CC – conditioning circuit, AI – analogue front end, DIO – digital input output, MCU – low power microcontroller, MEM – flash memory and R – IEEE802.15.4 transceiver

key feature in this type of measuring systems that are submitted to harsh working conditions. The implemented measuring channels are designed to provide the information regarding pollution (acid rain, polluted water discharge that can affect the values of conductivity from μS/cm to mS/cm) or to monitor estuarine tidal and associated natural phenomena by measurement of temperature, conductivity and turbidity parameters.

2.1 Conductivity measuring channel

The electrical conductivity of a water solution reflects the ability of the solution to conduct an electric current and it depends on the amount of ions present in the solution. In the present case, two-electrode cell architecture was implemented to perform conductivity measurements. One important parameter of cell is the so-called 'cell constant' which is the relation between the distance between the electrodes and their area determined by their geometric shape. The cell geometry was designed to allow a 0.1–20 mS/cm measuring range. The conductivity measuring channel includes two main sub-circuits, one that contains an oscillator, an active bridge amplifier and a difference amplifier, and the other sub-circuit that contains a precision half-wave rectifier, a low-pass filter and a non-inverter amplifier. Both sub-circuits, 1 and 2, are represented in Figs. 2 and 3, respectively.

In order to avoid the polarisation phenomena and to minimise double layer effects [17, 18], the voltage applied
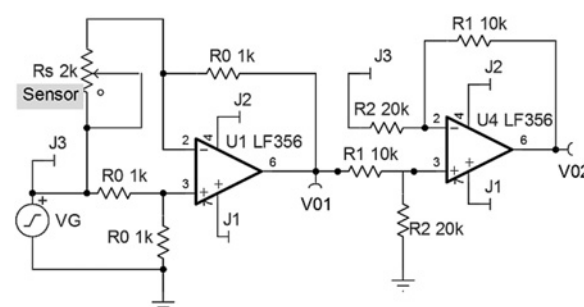

Fig. 2 *Conductivity signal conditioning: sub-circuit 1*
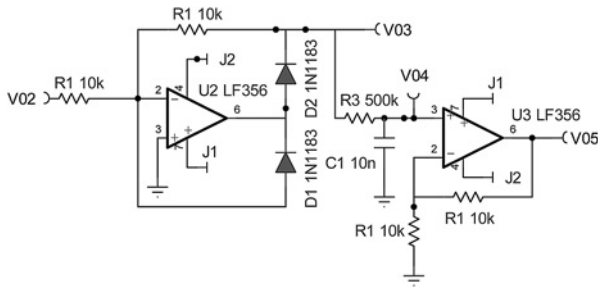Wheatstone bridge amplifier and difference amplifier

Fig. 3 *Conductivity signal conditioning: sub-circuit 2*

Precision half-wave rectifier, low-pass filter and signal amplifier

Fig. 4 *Voltage waveforms obtained in different voltage pins of the conditioning circuit for a sensor resistance value equal to 250 Ω*

V_G – oscillator output voltage; V_{01} – output voltage from the Wheatstone bridge amplifier; V_{03} – precision half-wave rectifier output voltage; V_{04} – low-pass filter output voltage and V_{05} – non-inverter amplifier output voltage

to the electrodes is sinusoidal and has a frequency of 5 kHz. This sinusoidal signal is generated by a Wien bridge oscillator whose output voltage is labelled as VG1 in sub-circuit 1. Considering that all electrical components are ideal, the output voltage from the Wheatstone bridge amplifier is given by

$$V_{01}(t) = \left(1 - \frac{R_0}{R_S}\right) \cdot \frac{V_G(t)}{2} \qquad (1)$$

where R_0 represents a reference resistor value, in the present case equal to 1 kΩ, R_S represents the conductivity cell resistance and V_G represents the Wien bridge oscillator output voltage.

Using the gain coefficients of the difference circuit relatively to each input and (1), it is possible to obtain the output voltage of sub-circuit 1

$$V_{02}(t) = \frac{V_G(t)}{2} \cdot \frac{R_0}{R_S} \qquad (2)$$

Regarding sub-circuit 2 that contains a low-filter with a cut-off frequency approximately equal to 30 Hz, which is much lower than signal frequency, it is possible to obtain the output voltage of the signal conditioning circuit that is given by

$$V_{05} = \frac{(V_G)_{ef}}{2 \cdot \beta_S} \cdot \frac{R_0}{R_S} \qquad (3)$$

where $(V_G)_{ef}$ represents the r.m.s. value of the oscillator output voltage, β_S represents the waveform factor of a sinusoidal wave and the other variables have the same meaning that was previously defined.

Hence, considering that R_S and R_0 can be expressed as

$$\begin{cases} R_S = \dfrac{1}{\sigma_S} \cdot CC \\[2mm] R_0 = \dfrac{1}{\sigma_0} \cdot CC \end{cases} \qquad (4)$$

where CC represents the cell constant and σ_0 the reference conductivity value that is associated with R_0, the output voltage from sub-circuit 2 (V_{05}) is given by

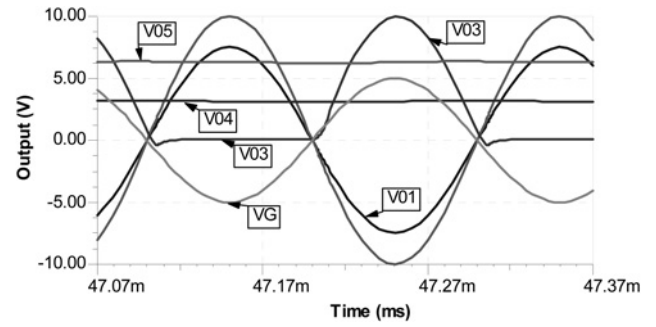$$V_{05} = \frac{(V_G)_{ef}}{2 \cdot \beta_S \cdot \sigma_0} \cdot \sigma_S \qquad (5)$$

This relation expresses a linear dependence between the conditioning circuit output voltage and conductivity.

Concerning simulation results, Fig. 4 represents the voltage waveforms that are obtained in different testing points of the conditioning circuit when the sensor resistance is equal to 250 Ω, which means $G_S = 4$, where G represents conductance. From the figure, it can be confirmed that all voltage waveforms and correspondent amplitudes agree with the theoretical expectations, and particularly the amplitude of the output voltage of the circuit (V_{05}), from which conductivity is evaluated, is equal to 6.3 V, which corresponds to a relative deviation from the theoretical value lower than 0.5%.

Fig. 5 represents the output voltage of the conditioning circuit for a set of four different conductance values, namely, for $G = 1, 2, 3$ and 4 mS.

The graph confirms the expected linear dependence between the conditioning circuit output voltage and conductance. A linear correlation between these variables was performed and a correlation coefficient approximately equal to 0.99 was obtained. Thus, the simulation results presented in Fig. 5 and the experimental results that were performed confirmed that the proposed conditioning circuit provides a constant sensitivity over the conductivity measuring range, being the conductivity evaluation inverse model expressed by a constant coefficient. Furthermore, the circuit allows to easily adjust the conductivity measurement dynamic range by selecting an appropriate value of the reference resistance (R_0) or by using a programmable gain amplifier connected to the output of the low-pass filter, being possible to avoid very low or very high output
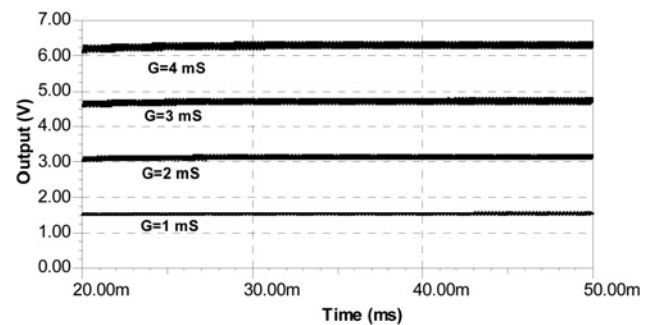

Fig. 5 *Output voltage of the conditioning circuit for four conductance values*

$G = 1, 2, 3$ and 4 mS

voltages of the signal conditioning circuit that irremediably affect the signal-to-noise ratio of the conductivity measuring circuit.

2.2 Temperature measuring channel

The temperature measuring channel is based on an NTC thermistor. The conditioning circuit combines a resistive divider and a non-inverter amplifier based on the LM324 circuit. If required, the non-linear characteristic of the thermistor can be linearised using an A/D converter [19, 20]. This linearisation can be accomplished using an A/D whose non-linear characteristic is adjusted to give a transfer characteristic that is the inverse of the thermistor characteristic.

Taking into account the temperature influence on conductivity measurement, the temperature measurement value is used to compensate conductivity variations caused by temperature variations. Thus, the conductivity measured values are always referenced to a reference temperature, typically equal to 25°C. Assuming a linear relationship between conductivity and temperature, which is always valid for small temperature range variations, the relationship between measured and temperature compensated values is given by

$$\sigma_{T0} = \frac{\sigma}{1 + \alpha \cdot (T - T_0)} \qquad (6)$$

where σ and σ_{T0} represent the measured and temperature compensated conductivity values, respectively, T and T_0 represent the temperature and reference temperature values, respectively, and α represents the coefficient of conductivity variation with temperature.

2.3 Turbidity measuring channel

Turbidity can be defined as an 'expression of the optical property that causes light to be scattered and absorbed rather than transmitted in straight lines through the sample' [16]. The set-up used for turbidity measurement is based on a sensing cell that includes two infrared emitter diodes to generate the infrared beams and two photodiodes to detect the transmitted and scattered light. It is important to refer that ultra-violet or visible light wavelengths must not be used in order to avoid errors caused by solution absorbance variations, namely by solution colour variations. The on–off control of the conditioning circuit associated with the emitter diodes is done by DIO port of the WQ sensing node (see Fig. 6). Appropriate conditioning circuitry is
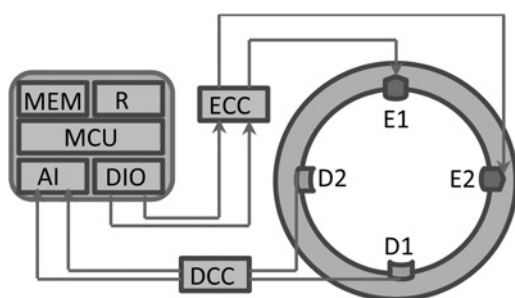
implemented for the detection diode, the voltage output being applied to the AI block of the WQ sensing node. The sensor control is done by embedded software that assures the proper on–off timing in such way that only one LED is switched-on at a time. According to the diagram of Fig. 6, the infrared LED conditioning circuit, ECC, is controlled using two digital output lines of the WSN-3202 module, while the output voltages of the detectors conditioning circuits are acquired by two of the analogue input channels of the above mentioned module.

When 'E1' is active for a short period of time (0.5 s), the detected lights measured by 'D1' and 'D2' are acquired by the system. Then 'E1' is switched-off and 'E2' is switched-on also for the same period of time, and new values of 'D1' and 'D2' are acquired. The measured voltage values associated with transmitted and scattered light are used to calculate the turbidity coefficient (C_m) given by

$$C_m = \pm \sqrt{\frac{V_{21}}{V_{11}} \times \frac{V_{12}}{V_{22}}} \qquad (7)$$

where V_{11} is the voltage detected by 'D$_1$' with 'E$_1$' active, V_{12} is the voltage detected by 'D$_2$' with 'E$_1$' active, V_{21} is the voltage detected by 'D$_1$' with 'E$_2$' active and finally V_{22} is the voltage detected by 'D$_2$' with 'E$_2$' active. The conversion C_m to turbidity conversion is done using the $C_m = C_m(TU)$ characteristic experimentally obtained for a set of formazine turbidity calibration solutions. The C_m calculation and C_m to TU conversion are performed by the MCU of WQ sensing node.

2.4 Wireless sensor network

The I/O and wireless communication module is expressed by NI WSN-3202 as part of a ZigBee network [21, 22]. The module can be configured as router (R) or end node (E) using the NI MAX utility.

The main specifications of the wireless sensing nodes with multifunction capabilities are: four analogue inputs (±10, ±5, ±2 and ±0.5 V range), 16 bit resolution and minimum sample interval 1 s, four DIO lines. The communication between the host computer and the network nodes (end nodes WQ-WSN-Ei, and routing nodes WQ-WSN-Ri) is performed through the usage of NI WSN-9791 wireless sensor network Ethernet gateway (WSN-G) (Fig. 7).

Considering the limited ranges (up to 300 m) of the wireless communication module, a 2.4 GHz high gain
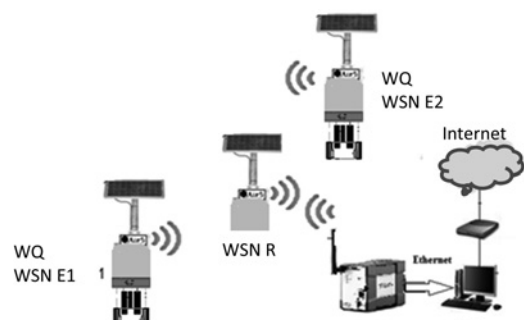

Fig. 6 *Diagram of the turbidity measuring system*
ECC – emitters conditioning circuit, DCC – detectors conditioning circuit; D1 and D2 optical detectors; E1 and E2 optical emitters; AI – analogue inputs; DIO – digital input output port

Fig. 7 *WQ wireless sensor network architecture*
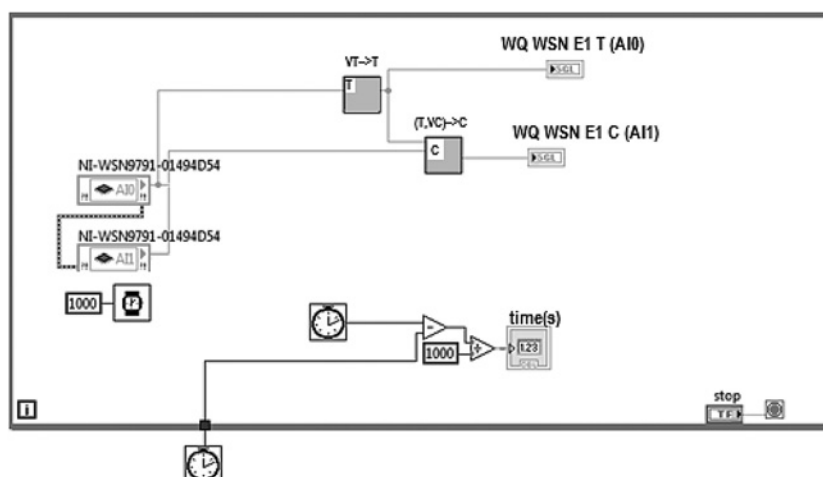WQ-WSN-E1, WQ-WSN-E2 – WQ end nodes, WSN-R – routing node and WSN-G – gateway

Fig. 8 *WQ-WSN-E1 LabVIEW implementation of data acquisition, processing based on shared variable associated with the WSN-E1 of the T and C measuring channels*

antenna (15 dBi) was used together with the WSN Ethernet gateway, which assures better coverage and permits to increase the distance between the gateway and the routing node (WSN-R). Because of their power consumption, the WSN measuring nodes are also part of an energy harvesting application based on a solar panel [23].

3 System software

The system software has two components: embedded LabVIEW software associated with WQ-WSN-E1 and E2, and host computer LabVIEW software that receives the values from the sensor nodes and performs data logging and web publishing based on LabVIEW server capabilities.

The development of the first component was done using LabVIEW WSN that permits to configure the wireless sensor network and also to manage sensor data through the use of shared variables associated with the analogue input channels (AI0, AI1, AI2 and AI3) and digital lines (DIO0, DIO1 and DIO2).

The data from the sensors is processed using a set of polynomial inverse models of WQ measuring channels as part of the WSN node firmware or as a component of the server application. Usually, the software module performs the voltage-to-physical quantity conversion (e.g. voltage to temperature expressed in °C; voltage to turbidity expressed in NTU).

The easy way to perform the acquisition of the WQ information is based on the default firmware installed on the WSN node that corresponds to the polling functioning mode. In this mode, the WQ-WSN node transmits every acquired sample back to the gateway (WSN-G) at a fixed sample rate (e.g. 1 sample each 30 s), the sampling rate being adapted to the variation of the monitored quantities and also to the requirements concerning the battery consumption.

A particular implementation associated with WQ-WSN-E1 is presented in Fig. 8. In the figure can be observed that for the particular case of T (temperature) and C (water electrical conductivity), two inputs–one output sensor inverse modelling modules were considered taking into account the influence of temperature on the C measuring channel characteristics.

The above mentioned acquisition scheme is easy to be implemented using the default firmware but implies less

autonomy of WSN nodes when the sampling rate is high (e.g. sampling rate = 1 s). Using the LabVIEW WSN the node firmware may be customised to extend the node battery life through sampling rate control and imposing appropriate moments to transmit data from the nodes to the gateway.

To extend the battery life, an implementation of a logic scheme at the WSN firmware level was considered in order to optimise the node behaviour for specific operating conditions or network requirements. For example, if the battery voltage decreases to a critical level (e.g. 2.5 V), the node will send a notification to the server application using a Boolean variable followed by decreasing its sampling and transmission rate to conserve the remaining battery life.

4 Experimental results

For accurate measurement of WQ conditions the measuring channel associated with WQ-WSN must be previously calibrated and tested. In the conductivity measuring channel case, a reference conductivity measuring instrument that uses the same conductivity measuring cell was used. The values of conductivity indicated by the reference measuring system were associated to the voltages acquired (V_c) from the nodes conductivity measuring channels for water samples with different values of conductivity. This method allowed obtaining the characteristic curve for the conductivity measuring channel that is presented in Fig. 9. Using a polynomial inverse model, the conductivity values
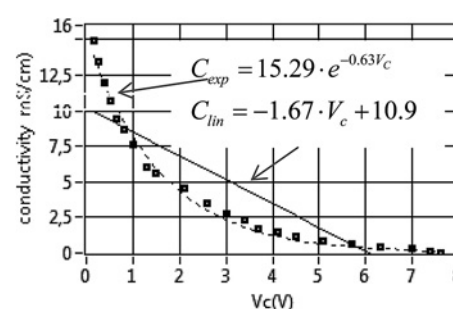

Fig. 9 *Characteristic curve of a conductivity input channel*

-- C_{lin} is the linear approximation, -.- C_{exp} is the exponential approximation and V_C – is the acquired voltage on conductivity measuring channel for different conductivity standard solutions
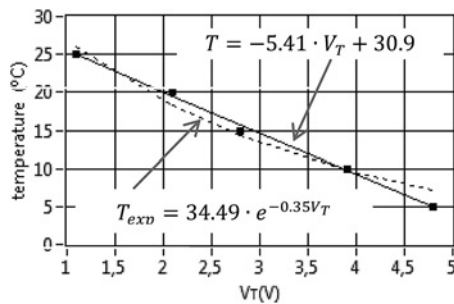
Fig. 10 *Characteristic curve of a temperature input channel*

V_T – acquired voltage on temperature channel for different standard temperatures

are calculated from the voltage values output by the conductivity measuring channels.

The temperature characteristic curve in Fig. 10 was obtained using an oven with temperature control to impose the calibration points and to obtain the data required to calculate the linear regression of the temperature measuring channels characteristic.

For the calibration of the turbidity measuring channels, four formazin turbidity standard solutions of 10, 100, 200 and 400 NTU were used, since formazin solutions are reference material for turbidity instrument calibration. After the turbidity coefficients are calculated, the turbidity characteristic curve and the corresponding linear approximation are obtained (Fig. 11).

Based on calibrated measuring channels associated to each WQ-WSN-Ei, several measurements and data communication tests were carried out. The values of the conductivity measuring channel with temperature compensation associated to WSN-E1 obtained in a laboratory measuring session are presented in Table 1. The accuracy obtained was 2% FS (0–15 mS/cm).
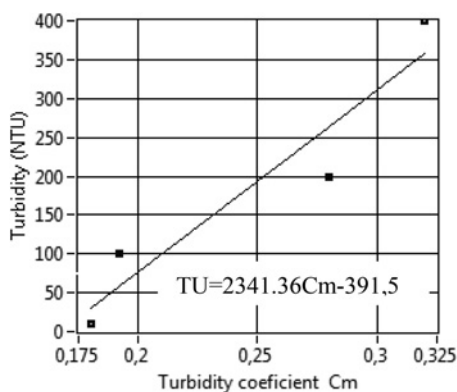

Fig. 11 *Characteristic curve of a turbidity measuring channel*

Table 1 Conductivity results (full-scale: 15 mS/cm)

Percentage of span, %	Ref. value, µS/cm	Measured value, µS/cm	Error, % FS
0	0	90	1
25	3930	3827	1
50	7610	7698	1
75	11 520	11 594	1
100	15 000	15 368	2

Tests on temperature and turbidity measuring channels revealed accuracy values of 1% FS (5–25°C) and 5% FS (0–400 NTU), respectively.

5 Conclusions

This paper presents the design and implementation of surface water real-time monitoring based on a ZigBee wireless sensor network.

An important part of the work includes the development of a low cost multi-parameter WQ measuring probe attached to the wireless sensor node. Thus, it was designed, implemented and tested a conductivity measuring channel characterised by a two-electrode cell in combination with a temperature measuring channel. The proposed conditioning circuit used in conductivity measuring channel is based on a Wheatstone bridge amplifier and provides an output voltage that linearly depends on conductivity. The probe also includes a turbidity measuring channel whose working principle is based on a set of two infrared optical emitters and detectors pairs that provide the detection of the transmitted and scattered light caused by the particles in suspension in the water. The limited number of WQ measurement sensors associated with wireless sensor nodes and the necessity to perform periodic verification/calibration of the sensors can be considered as a drawback of the presented solution. The last problem can be solved with the inclusion of an in-situ calibration system associated with WQ measuring channels. A prototype of this kind of system was developed and reported by the authors in the past. The inclusion of a field calibrator will imply additional costs and will affect the autonomy of the distributed measurement system of WQ parameters.

The laboratory tests of the implemented WQ-WSN proved the capability of the system to provide accurate WQ information. Future developments of the proposed measurement system will consider the inclusion of additional sensing devices and the analysis of reliability issues related with the usage of other conductivity cell types, such as, four electrode or inductive cells, that are less sensitive to external working conditions.

6 References

1 IBM, Smarter Cities, on-line at http://www.ibm.com/smarterplanet/us/en/smarter_cities/overview/index.html
2 Postolache, O., Girão, P.S., Ferraria, G., Barroso, N., Pereira, J.M.D., Postolache, G.: 'Indoor monitoring of respiratory distress triggering factors using a wireless sensing network and a smart phone'. Int. Instrumentation and Measurement Technology Conf. 2009 (I2MTC'2009), Singapore, May 2009, pp. 451–456
3 Stiel, I.G., Spaite, D.W., Field, B., et al.: 'Advanced life support for out-of hospital respiratory distress', *NEJM*, 2007, **356**, (24), pp. 2156–64
4 Rabe, K.F., Hurd, S., Anzuento, A., et al.: 'Global strategy for the diagnosis management, and prevention of chronic obstructive pulmonary disease: GOLD executive summary', *Am. J. Respir. Crit. Care Med.*, 2007, **176**, (6), pp. 532–55
5 Indoor air quality impacts child asthma, Humidex Reduces contaminates that trigger asthma attacks: http://www.naturalnews.com/010255.html
6 Tomizuka, M., Yun, C.B., Giurgiutiu, V.: 'A smart indoor air quality sensor network'. Proc. SPIE, Smart Structures and Materials, 2006, vol. 6174, pp. 1277–1290
7 Ulivieri, N., Distante, C., Luca, T., Rocchi, S., Siciliano, P.: 'IEEE1451.4: a way to standardize gas sensor', *Sensors Actuators B, Chem.*, 2006, **114**, (1), pp. 141–151
8 Bielsa, A.: 'Libelium world:smart city project in Salamanca to monitor air quality and urban traffic', available at: http://www.libelium.com/smart_city_air_quality_urban_traffic_waspmote/

9   Postolache, O., Pereira, J.M.D., Girão, P.: 'Smart sensors network for air quality monitoring applications', *IEEE Trans. Instrum. Meas.*, 2009, **58**, (9), pp. 3253–3261

10 González, C.M., Aristizábal, B.H.: 'Acid rain and particulate matter dynamics in a mid-sized Andean city: the effect of rain intensity on ion scavenging', *Atmos. Environ.*, 2012, **60**, pp. 164–171

11 Beverland, I.J., Heal, M.R., Crowther, J.M., Srinivas, M.S.N.: 'Real-time measurement and interpretation of the conductivity and pH of precipitation samples', *Water Air Soil Pollut.*, 1997, **98**, (3-4), pp. 325–344

12 Coren, M.J.: 'The air quality egg will let you know exactly what you're breathing' available at: http://www.fastcoexist.com/1679740/the-air-quality-egg-will-let-you-know-exactly-what-youre-breathing

13 'Hydrolab Quanta Multiparameter Sonde', http://www.hachhydromet.com/web/ott_hach.nsf/id/pa_quanta.html, 2012

14 'Rosemount Analytical Model 1057 Multiparameter Analyser', www2.emersonprocess.com/en-US/brands/rosemountanalytical/Liquid/

15 Torrent, J.: 'Low-cost conductivity cells for water measurement purposes'. IMTC 2004–Instrumentation and Measurement Technology Conf., Como, Italy, 18–20 May 2004

16 Postolache, O., Girão, P., Pereira, J.D., Ramos, H.G.: 'Multibeam optical system and neural processing for turbidity measurement', *IEEE Sensors J.*, 2007, **7**, (5), pp. 677–684

17 Mutoh, N., Inoue, T.: 'A control method to charge series-connected ultraelectric double-layer capacitors suitable for photovoltaic generation systems combining MPPT control method', *IEEE Trans. Ind. Electron.*, 2007, **54**, (1), pp. 374–383

18 Korthum, G.: 'Treatise on electrochemistry' (University of Tubingen, Germany, 2nd edn. by American Elsevier Publishing, New York, 1965)

19 Pereira, J.M.D., Postolache, O., Girão, P.: 'PWM-A/D conversion: a flexible and low-cost solution for transducer linearization'. Proc. ISA/IEEE – SIcon01, Rosemount, Illinois, EUA, November 2001, pp. 258–263

20 Pereira, J.M.D., Postolache, O., Girão, P.S.: 'A digitally programmable A/D converter for smart sensors applications', *IEEE Trans. Instrum. Meas.*, 2007, **56**, (1), pp. 158–163

21 ZigBee Alliance, Control your world, available at: http://www.ZigBee.org

22 Pereira, J.M.D., Postolache, O., Girão, P.: 'Spread spectrum techniques in wireless communication', *IEEE Instrum. Meas. Mag.*, 2009, **12**, (6), pp. 21–24

23 Postolache, O., Pereira, J.M.D., Girão, P.M.: 'Geenhouses microclimate real-time monitoring based on a wireless sensor network and GIS'. Proc. IMEKO World Congress, Busan, Korea, South, September 2012, Vol. 1, pp. 1–5